


Destruction threshold of ZrO₂ under microsecond magnetic-pulse action

S.I. Krivosheev, G.A. Shneerson , S.G. Magazinov , D.V. Zhukov, K.V. Voloshin 

Peter the Great St. Petersburg Polytechnic University, St. Petersburg, Russia

 magazinov_sg@mail.ru

Abstract. The paper describes the magnetic pulse method for the formation of controlled pressure pulses in a microsecond range of duration for testing the dynamic mechanical strength of brittle materials. The scheme of the experimental setup includes a pulse current generator (PCG), the magnetic pulse loading system, the pulse current measuring system and the sample. The main parameters of the developed experimental setup are given - charging voltage, capacitance, inductance, active resistance of the PCG. Zirconium dioxide samples were tested according to this method. Numerical simulation of pulsed magnetic and dynamic mechanical fields during testing of materials is performed. Experimental pulses of the generated pressure are calculated. Based on the results of experiments and numerical modeling, the dynamic mechanical strength of zirconium dioxide under loading mode I was determined based on the described method.

Keywords: pulsed magnetic fields; magnetic pulse loading; high strain rate deformation; testing of materials

Acknowledgements. *This work was supported by the Russian Science Foundation (grant no. 18-19-00230). The results of the work were obtained using the computing resources of the supercomputer center of Peter the Great St. Petersburg Polytechnic University.*

Citation: Krivosheev SI, Shneerson GA, Magazinov SG, Zhukov DV, Voloshin KV. Destruction threshold of ZrO₂ under microsecond magnetic-pulse action. *Materials Physics and Mechanics*. 2023;51(7): 7-14. DOI: 10.18149/MPM.5172023_2.

Introduction

Large current and power loads, typical for the operation of high-powered electrophysical installations, require consideration of the strength properties of all elements that make up the equipment and operate under conditions of combined effects. So, when generating strong pulsed magnetic fields, current-carrying elements (coils of the solenoid) experience the action of Lorentz forces and Joule heating, and the insulation that separates them experiences mechanical and thermal loads and the effect of applied impulse voltage. The stress state in these systems is quite complex, and the performance of the solenoid is determined by limiting current loads, which determine the choice of material of the coils, and by the properties of the insulation, which ensures the electrical strength of the structure. In this case, the insulation can perform the function of containing deformations of current-carrying elements. Examples are the designs of solenoids with quasi-forceless windings described in [1,2], the mechanical stresses in which are significantly reduced with an increase in the elastic modulus of the material filling the inter-turn gaps. Therefore, it is of interest to study the strength characteristics of media having a high modulus of elasticity (ceramic dielectrics) under loading conditions close to those realized in magnets with a pulsed field. An example would be a magnet with inertial confinement of the screen, which balances its front-end part, described in [3]. The

magnet (Fig. 1) is designed to obtain a magnetic field in a small volume in the form of a pulse with a duration of 10 μs and an induction amplitude of up to 50 T. Numerical simulation showed that in the insulation between the winding coils, the mechanical stress calculated by the von Mises criterion, can reach 1 GPa.

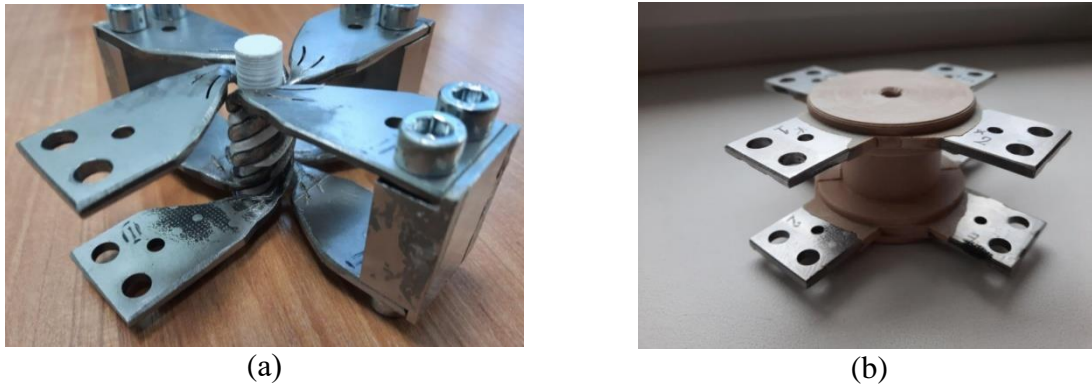


Fig. 1. Solenoid with quasi-forceless windings: (a) coils; (b) insulation of coils

This article describes an installation designed to generate controlled pressure pulses and an experimental-calculation method for determining the threshold breaking load of a dielectric in the microsecond range of exposure durations.

Testing of the installation was carried out during testing of zirconium dioxide. In the experiments described, the pressure wave front propagation time to the edge of the sample is commensurate with the pulse duration; therefore, a necessary part of the work was the use of computer simulation to calculate the mechanical stress, taking into account the process of formation and propagation of the pressure wave.

It is known that the mechanical properties of materials, such as the elastic limit, hardening factor [4–10] and tensile strength depend on the deformation rate of materials. There are various methods for testing the dynamic properties of materials [11–14], but the loading schemes used in these methods are very conservative and cannot be used in sample configurations that are not traditional for these methods. A magnetic-pulse method [15–22] for the formation of shock loads is used in this work. The material under study in this work (zirconium dioxide) does not have pronounced plastic properties and its deformation characteristic can be represented as a linear dependence of mechanical stresses on relative deformations, therefore, the main interest in determining the mechanical properties of zirconium dioxide is its dynamic strength limit, in the time range, close to operating conditions of the solenoid.

Methods

Formation of controlled pressure pulses. To study the dynamic tensile strength, this work uses a magnetic-pulse technique for generating controlled pressure pulses [19–21], adapted to testing materials with a high tensile strength, a simplified diagram of which is shown in Fig. 2.

In the above test scheme, there are three blocks: a pulsed currents generator (PCG) I, a Rogowski coil II, a magnetic-mechanical loading system III, and a test sample 2.

The geometric dimensions of the tested zirconium dioxide specimens are: length 23 mm, width 23 mm, thickness 8 mm, groove length 15 mm, groove height 3 mm, groove top rounding radius 1.5 mm. Sample elasticity modulus $E = 210$ GPa, density $\rho = 6200$ kg/m³.

The pulsed currents generator (PCG) I consists of impulse capacitors with a total capacity of $T_{PCG} = 30$ μF , a charging voltage of up to 25 kV, a low-inductance busbar $L_{PCG} = 75$ nH and a controlled spark gap S_{PCG} , made of two parallel thyratrons of the TDI4-250k / 20PE type with a control unit PB-3DV/2E.

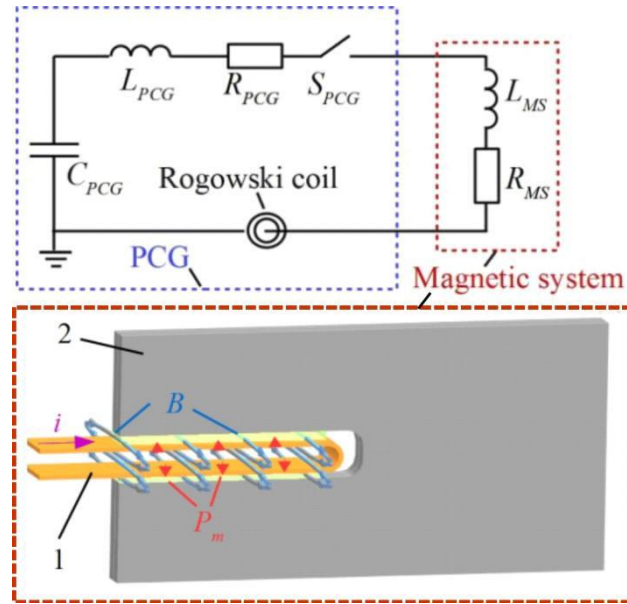


Fig. 2. Scheme of magnetic-pulse testing of the dynamic tensile strength of materials:

1 - copper flat busbars, 2 - test sample

The Rogowski coil II is connected through an integrating RC-circuit with an integration constant much longer than the measured signal to the input of oscilloscope to record the PCG discharge current.

Loading system III is made of flat closely spaced copper bifilar busbars, 0.3 mm thickness, 10 mm width. There is a groove in the sample with flat copper busbars placed.

After the PCG capacitors are charged to a predetermined voltage level, using a controlled spark gap, the PCG is discharged onto copper bars, where pulsed magnetic field is formed. The magnetic field interacts with the flat busbar current and generates a pulsed magnetic pressure, which is transferred to the edges of the sample's groove. Under the influence of this pressure, the sample's groove opens, which leads to the formation of a region of maximum mechanical stresses at the top of the groove.

By adjusting the charging voltage of capacitors and/or the width of the copper busbars of the magnetic-mechanical loading device, it is possible to vary the amplitude of magnetic pressure acting on the sample. The charging voltage and busbars width corresponding to the sample destruction threshold are experimentally determined. The charging voltage corresponding to the threshold voltage is the voltage, below which the destruction of sample is not observed, and with an increase in voltage, the destruction of sample occurs. During the discharge, pulsed current is measured. With the help of numerical simulation, the mechanical stress at the top of the sample is determined, which corresponds to dynamic tensile strength for a given form of loading.

A typical experimental oscillogram of the current of test setup in the short circuit mode is shown in Fig. 3.

The current pulse is approximated by the following expression:

$$i(t) = I_m \cdot \sin(2\pi/T \cdot t) \cdot \exp(-t/\tau), \quad (1)$$

where $I_m = U_0/\rho$ - maximum current value without attenuation, $\rho = \sqrt{L/C} = 50 \text{ M}\Omega$ is the wave resistance, $T = 2\pi\sqrt{LC} = 9.5 \text{ ms}$ is the period of oscillation, $\tau = 21 \text{ ms}$ is the attenuation constant.

The charging voltage of the test set can be changed in the range $U_0 = 5 \dots 25 \text{ kV}$ which corresponds to $I_m = 100 \dots 500 \text{ kA}$.

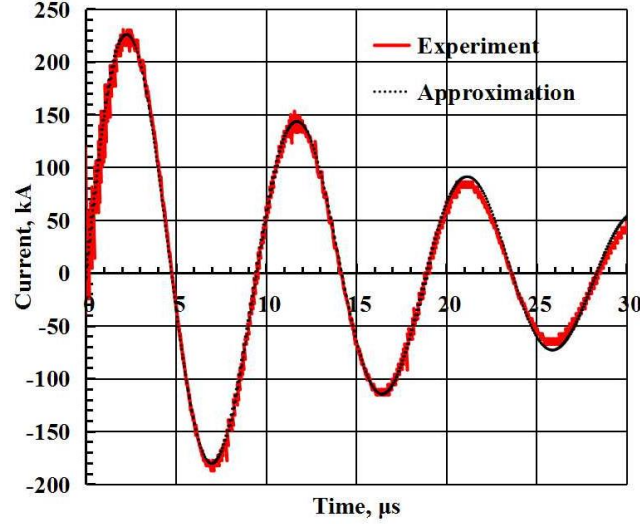


Fig. 3. Typical oscillogram of the experimental current

Flowing through the flat bifilar busbars, the pulsed current forms a pulsed magnetic field between them, which creates pressure on the busbars, determined by the expression:

$$P_m(t) = k_m \cdot \mu / 2 \cdot (i(t)/c)^2, \quad (2)$$

where c is the width of the flat busbars, k_m is a rate that is equal to 1 with a uniform distribution of current density in the busbars, which occurs if the width of the busbars is much larger than the gap between them. Under experimental conditions, the values of this coefficient lie in the range $k_m = 0.4 \dots 0.8$ and are determined by the results of numerical simulation of the magnetic field for given dimensions of flat busbars and pulsed current parameters.

Computer modelling. To determine the magnetic pressure coefficient k_m under experimental conditions, a numerical simulation of a pulsed magnetic field in the Comsol Multiphysics environment was performed with respect to the vector magnetic potential A , defined by the expression:

$$\Delta \bar{A} - \sigma \mu \frac{\partial \bar{A}}{\partial t} = \mu \bar{J}, \quad (3)$$

where σ, μ are the electrical conductivity and magnetic permeability respectively.

According to the known distribution of the vector magnetic potential, it is possible to determine all the parameters of the magnetic field, such as the magnetic field induction $\bar{B} = \nabla \times \bar{A}$, magnetic field strength $\bar{H} = \bar{B} / \mu$, current density $\bar{J} = \nabla \times \bar{H}$. The vector product of the magnetic field induction and the current density gives the vector of the volumetric Lorentz force $\bar{f}_L = \bar{J} \times \bar{B}$ acting on the copper bars. By integrating the vertical component of this force over the cross section of the conductor, the magnetic pressure of the magnetic-mechanical loading system is determined, which is transmitted to the edges of the sample's groove [23].

To determine the mechanical stresses at the top of the sample groove (the zone of maximum mechanical stresses), a numerical simulation of the dynamic mechanical field in the Comsol Multiphysics environment was performed based on Newton's second law in differential form with a linear deformation dependence determined by Hooke's law:

$$m \frac{\partial^2 \bar{u}}{\partial t^2} = \bar{f}_L - \nabla \cdot \bar{\sigma}, \quad (4)$$

$$\bar{\sigma} = E \cdot \bar{\varepsilon}, \quad (5)$$

where u is the vector of displacements, σ is the mechanical stress tensor, m is mass, ε is strain tensor, E is elastic moduli tensor.

Results

A series of experiments was carried out on samples of zirconium dioxide, the tire width in all experiments was kept constant and equal to 10 mm. The charging voltage of the test setup was empirically determined, corresponding to the sample destruction threshold $U_S = 6$ kV.

When the charging voltage decreased below U_S , the destruction of the samples was not observed, and the excess of the charging voltage above the U_S value led to the destruction of the samples (see Fig. 4).



Fig. 4. Samples after testing: (a) the charging voltage is less than the threshold; (b) the charging voltage is above the threshold

Based on the numerical simulation of the magnetic field, the magnetic pressure coefficient $k_m = 0.55$ was determined and the time dependences of the magnetic pressure acting on the sides of the samples' grooves were found. They are shown in Fig. 5(a).

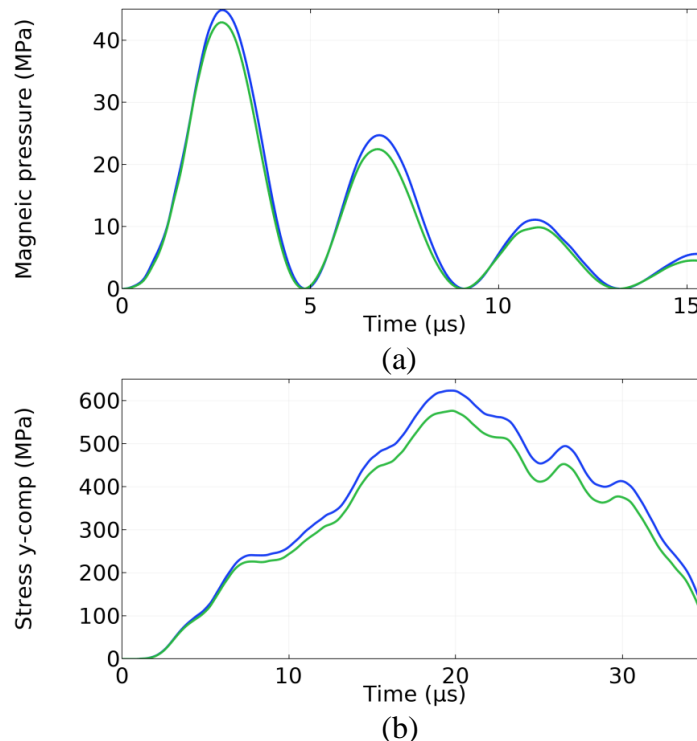


Fig. 5. Graphs of the dependences of the magnetic pressure (a) applied to the edges of the sample's groove and the calculated value of the y-component (tensile) of the mechanical stress (b) at the top of the sample's groove on time, close to the fracture threshold: blue curve - corresponds to the experiment with the destruction of the sample; green curve - without destruction of the sample

On the basis of numerical simulation of dynamic mechanical deformation of samples under the influence of pulsed pressure corresponding to the experimental conditions, the time dependence of tensile mechanical stress at the top of the groove, where it takes on a maximum value, was constructed (Fig. 5(b)).

The given data in Fig. 5(b) show that the amplitude of the threshold value of the y-component of mechanical stress of the tested samples is between the green curve corresponding to the experiment without sample destruction and the blue curve corresponding to the experiment with sample destruction. Thus, it can be argued that the threshold value under conditions of described experiments (for a pulse duration of 36 μs) is 600 ± 50 MPa.

3D modeling of the process has been completed. A spatial distribution of the y-component of stress tensor is shown Fig. 6(a) for one fourth of the sample. For the point at the top of the sample's groove in Fig. 6(b) shows the time dependences of x, y, z - the components of the stress tensor and the von Mises equivalent stress.

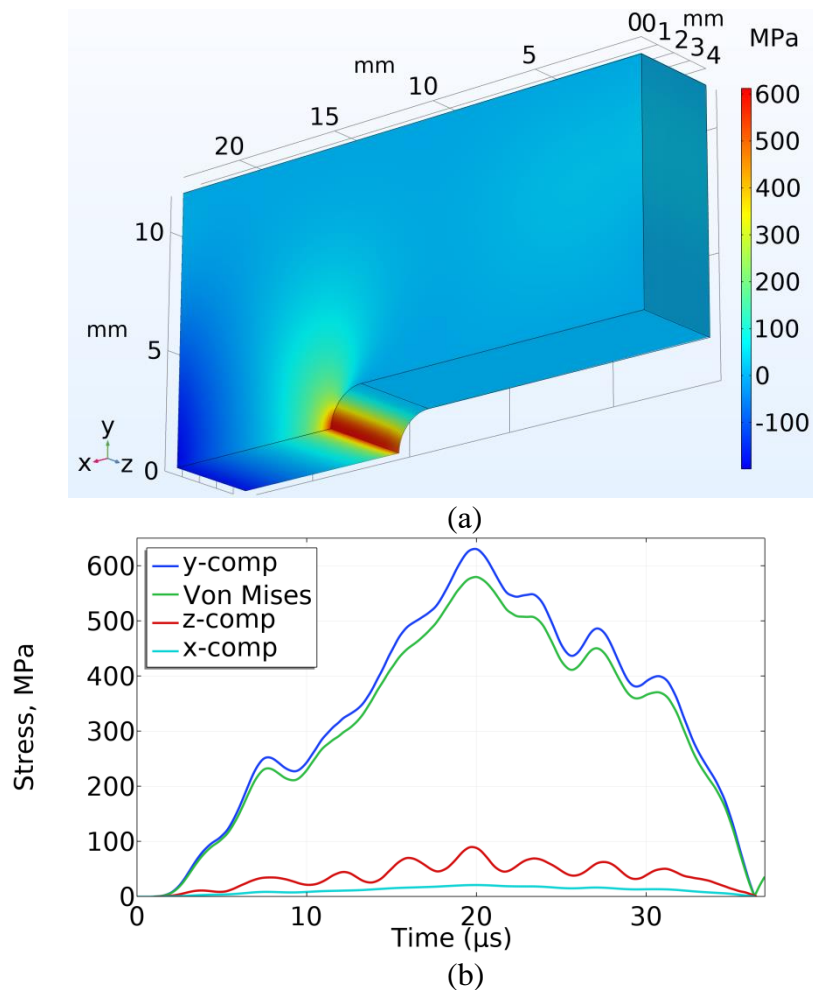


Fig. 6. Results of numerical simulation of dynamic deformation of samples under loading close to the fracture threshold: (a) distribution of the y-component of mechanical stresses (one fourth of the symmetry sample) at the time of maximum $t = 20 \mu\text{s}$; (b) time dependences x, y, z - components of the stress tensor and the equivalent stress at the top of the sample's groove

According to the results presented in Fig. 6, it can be seen that the mechanical wave length $\lambda = T \cdot (E/\rho)^{1/2} = 55$ mm is comparable to the characteristic dimensions of the samples ($23 \times 23 \times 8$ mm). The shape of the mechanical stress curves at the top of the groove does not repeat the shape of the applied magnetic pressure due to the dynamic nature of loading the edges of the groove with a uniformly distributed magnetic pressure. In this mode, at the top of the

slot, there is a superposition of stress waves formed under the influence of magnetic pressure on the entire slot boundary. The observed behavior of the dependences of stresses at the top of the groove observed in the calculations is related to the finite rate of stress propagation caused by the action on the sides of the groove, and corresponds to the description of similar processes under dynamic and shock-wave loading [24,25]. An analysis of the simulation results demonstrates the absence of a shock-wave nature of loading; therefore, we can assume that in our case, the loading mode of the samples is intermediate between wave and quasistatic.

From Fig. 6(b) it can be seen that the tensile y-component of the mechanical stress tensor dominates at the top of the sample's groove, the x and z components make up 3 and 14 % of the y-component, respectively. The von Mises stress at the top of the groove is 92 % of the y-component of the tensor.

Conclusion

Based on the testing of samples of zirconium dioxide, the possibility of testing the dynamic mechanical strength of materials in mode I by the magnetic pulse method was shown.

The dynamic tensile strength according to von Mises of the tested samples of zirconium dioxide when loaded by the magnetic-pulse method in mode I was 550 ± 50 MPa with a mechanical stress duration of 36 μ s.

References

1. Nemov AS, Lagutkina AD, Shneerson GA. A Conceptual 3-D Design of a Non-Destructive Two-Layer Quasi-Force-Free Magnet for Megagauss Field Generation. *IEEE Transactions on Magnetics*. 2022;3(58): 8000609.
2. Shneerson GA, Nemov AS, Lagutkina AD. Designing quasi-force-free configurations of non-destructive megagauss magnets. In: *Proc. 8th Euro-Asian Pulsed Power Conference (EAPPC 2020)*. 2020. p.1–26
3. Shneerson GA, Parfentyev AA, Titkov VV, Krivosheyev SI, Lagutkina AD, Nemov AS, Nenashev AP, Shimansky SA. Conceptual Model of a Quasi-Force-Free Magnet of Small Volume with Inertial Retention of Its End Part. *Tech. Phys. Lett.* 2021;47: 573–576.
4. Johnson GR, Cook WH. A constitutive model and data for metals subjected to large strains, high strain rates and high. In: *Proceedings of the 7th International Symposium on Ballistics Committee*. 1983. p.541–547
5. Follansbee PS, Kocks UF. A constitutive description of the deformation of copper based on the use of the mechanical threshold stress as an internal state variable. *Acta Metallurgica*. 1988;1(36): 81–93.
6. Zerilli FJ, Armstrong RW. Dislocation-mechanics-based constitutive relations for material dynamics calculations. *Journal of Applied Physics*. 1987;5(61): 1816–1825.
7. Preston DL, Tonks DL, Wallace DC. Model of plastic deformation for extreme loading conditions. *Journal of Applied Physics*. 2003;1(93): 211–220.
8. Korkmaz ME, Günay M, Verleysen P. Investigation of tensile Johnson-Cook model parameters for Nimonic 80A superalloy. *J. Alloys Compd.* 2019;801: 542–549.
9. Grazka M, Janiszewski J. Identification of johnson-cook equation constants using finite element method. *Eng. Trans.* 2012;60: 215–223.
10. Liu W, Zhou H, Li J, Meng Z, Xu Z, Huang S. Comparison of Johnson-Cook and Cowper-Symonds models for aluminum alloy sheet by inverse identification based on electromagnetic bulge. *Int. J. Mater. Form.* 2022;15: 10.
11. Kolsky H. An investigation of the mechanical properties of materials at very high rates of loading. *Proceedings of the Physical Society. Section B*. 1949;11(62): 676–700.
12. Novikov SA. Razrusheniye materialov pri vozdeystvii intensivnykh udarnykh nagruzok. *Sorosovskiy obrazovatelnyy zhurnal*. 1999;8: 116–121. (In-Russian)

13. Bragov AM, E. Kadoni LK. Sovremennyye metody dinamicheskikh ispytaniy materialov. *Vestnik Nizhegorodskogo universiteta im. N.I. Lobachevskogo*. 2011;5(4): 2039–2040. (In-Russian)
14. Taylor G. The use of flat-ended projectiles for determining dynamic yield stress. *Proceedings of the Royal Society of London A*. 1948;194: 289–299.
15. Nie H, Suo T, Wu B, Li Y, Zhao H. A versatile split Hopkinson pressure bar using electromagnetic loading. *Int. J. Impact Eng.* 2018;116: 94–104.
16. Avriel E, Lovinger Z, Nemirovsky R, Rittel D. Investigating the strength of materials at very high strain rates using electro-magnetically driven expanding cylinders. *Mech. Mater.* 2018;117: 165–180.
17. Zhang H, Ravi-Chandar K. On the dynamics of necking and fragmentation - I. Real-time and post-mortem observations in Al 6061-O. *Int. J. Fract.* 2006;142: 183–217.
18. Guo Y, Du B, Liu H, Ding Z, Zhao Z, Tang Z, Suo T, Li Y. Electromagnetic Hopkinson bar: A powerful scientific instrument to study mechanical behavior of materials at high strain rates. *Rev. Sci. Instrum.* 2020;91(8): 081501.
19. Krivosheev SI. Pulsed magnetic technique of material testing under impulsive loading. *Technical Physics*. 2005;3(50): 334–340.
20. Ostropiko E, Magazinov S, Krivosheev S. Uniaxial Magnetic Pulse Tension of TiNi Alloy with Experimental Strain Rate Evaluation. *Experimental Mechanics*. 2022;6(62): 1027–1036.
21. Magazinov SG, Krivosheev SI, Adamyan YE, Alekseev DI, Titkov VV, Chernenkaya LV. Adaptation of the magnetic pulse method for conductive materials testing. *Materials Physics and Mechanics*. 2018;40(1): 117–123.
22. Chandar KR, Knauss WG. Dynamic crack-tip stresses under stress wave loading -A comparison of theory and experiment. *International Journal of Fracture*. 1982;3(20): 209–222.
23. Ostropiko ES, Krivosheev SI, Magazinov SG. Analytical evaluation of magnetic pulse deformation of tini alloy. *Letters on Materials*. 2021;1(11): 55–60.
24. Krivosheev SI, Korovkin NV, Slastenko VK, Magazinov SG. Destruction of brittle materials by microsecond pressure pulses at their formation by magnetic pulse method. *International Journal of Mechanics*. 2015;9: 293–299.
25. Ma CC, Freund LB. The extent of the stress intensity factor field during crack growth under dynamic loading conditions. *Journal of Applied Mechanics, Transactions ASME*. 1986;2(53): 303–310.

THE AUTHORS

Krivosheev S.I.

e-mail: ksi.mgd@gmail.com

Shneerson G.A. 

e-mail: gashneerson@mail.ru

Magazinov S.G.

e-mail: magazinov_sg@mail.ru

Zhukov D.V.

e-mail: s_zhukov51@bk.ru

Voloshin K.V. 

e-mail: kir_vol@mail.ru